



Article

The Roles of Cullins E3 Ubiquitin Ligases in the Lipid Biosynthesis of the Green Microalgae *Chlamydomonas reinhardtii*

Qiulan Luo ¹, Xianghui Zou ¹, Chaogang Wang ², Yajun Li ³ and Zhangli Hu ^{2,*}

¹ School of Life Sciences and Food Engineering, Hanshan Normal University, Chaozhou 521041, China; luoqiulan_79@163.com (Q.L.); xzhui@hstc.edu.cn (X.Z.)

² Guangdong Technology Research Center for Marine Algal Bioengineering, Guangdong Provincial Key Laboratory for Plant Epigenetics, Shenzhen Engineering Laboratory for Marine Algal Biotechnology, Longhua Innovation Institute for Biotechnology, College of Life Sciences and Oceanography, Shenzhen University, Shenzhen 518060, China; charlesw@szu.edu.cn

³ Hainan Provincial Key Laboratory for Functional Components Research and Utilization of Marine Bio-Resources, Institute of Tropical Bioscience and Biotechnology, Hainan Academy of Tropical Agricultural Resource, Chinese Academy of Tropical Agricultural Sciences, Haikou 517010, China; liyajun_1980@163.com

* Correspondence: huzl@szu.edu.cn; Tel.: +86-755-26-557-312

Abstract: Microalgae-based biodiesel production has many advantages over crude oil extraction and refinement, thus attracting more and more concern. Protein ubiquitination is a crucial mechanism in eukaryotes to regulate physiological responses and cell development, which is highly related to algal biodiesel production. Cullins as the molecular base of cullin-RING E3 ubiquitin ligases (CRLs), which are the largest known class of ubiquitin ligases, control the life activities of eukaryotic cells. Here, three cullins (CrCULs) in the green microalgae *Chlamydomonas reinhardtii* were identified and characterized. To investigate the roles of CrCULs in lipid metabolism, the gene expression profiles of CrCULs under nutrition starvation were examined. Except for down-regulation under nitrogen starvation, the CrCUL3 gene was induced by sulfur and iron starvation. CrCUL2 seemed insensitive to nitrogen and sulfur starvation because it only had changes after treatment for eight days. CrCUL4 exhibited an expression peak after nitrogen starvation for two days but this declined with time. All CrCULs expressions significantly increased under iron deficiency at two and four days but decreased thereafter. The silencing of CrCUL2 and CrCUL4 expression using RNAi (RNA interference) resulted in biomass decline and lipids increase but an increase of 20% and 28% in lipid content after growth for 10 days, respectively. In CrCUL2 and CrCUL4 RNAi lines, the content of fatty acids, especially C16:0 and C18:0, notably increased as well. However, the lipid content and fatty acids of the CrCUL3 RNAi strain slightly changed. Moreover, the subcellular localization of CrCUL4 showed a nuclear distribution pattern. These results suggest CrCUL2 and CrCUL4 are regulators for lipid accumulation in *C. reinhardtii*. This study may offer an important complement of lipid biosynthesis in microalgae.

Keywords: *Chlamydomonas reinhardtii*; cullin; lipid metabolic; RNA inference; fatty acid



Citation: Luo, Q.; Zou, X.; Wang, C.; Li, Y.; Hu, Z. The Roles of Cullins E3 Ubiquitin Ligases in the Lipid Biosynthesis of the Green Microalgae *Chlamydomonas reinhardtii*. *Int. J. Mol. Sci.* **2021**, *22*, 4695. <https://doi.org/10.3390/ijms22094695>

Academic Editor: Leszek A. Kleczkowski

Received: 7 April 2021

Accepted: 27 April 2021

Published: 29 April 2021

Publisher's Note: MDPI stays neutral with regard to jurisdictional claims in published maps and institutional affiliations.



Copyright: © 2021 by the authors. Licensee MDPI, Basel, Switzerland. This article is an open access article distributed under the terms and conditions of the Creative Commons Attribution (CC BY) license (<https://creativecommons.org/licenses/by/4.0/>).

1. Introduction

Biodiesel from microalgae as a third generation biofuel has attracted growing attention because of its unique advantages such as a high efficiency for photosynthesis, the utilization of wastewater and the occupancy of less land [1]. Culture cost constitutes a large part of microalgae biodiesel production; therefore, numerous research has been performed to enhance the lipid and biomass production in microalgae by genetic engineering. Under abiotic stresses such as the deprivation of nutrients, microalgae accumulate lipids in the form of triacylglycerol (TAG), which is the main component of biodiesel [2]. To date, two TAG synthesis pathways have been found in microalgae; i.e., the Kennedy pathway and phospholipid: diacylglycerol acyltransferase (PDAT) mediated TAG synthesis [3]. In *C. reinhardtii*, the key enzymes involved in the Kennedy pathway were revealed in prior

years including diacylglycerol acyltransferase (DGAT), glycerol-3-phosphate acyltransferase (GPAT) and Glycerol-3-phosphate dehydrogenases (GPDH) [4–6]. Increasing or silencing the expression of the above genes has been applied to improve lipid content and indeed made certain achievements. For example, DGAT homologue genes, which have been demonstrated to play important roles in the TAG accumulation in higher plants, have distinct roles in microalgae. The overexpression of five *Chlamydomonas* DGAT2 genes showed only CrDGAT2-1 and CrDGAT2-5 could slightly increase the TAG content in cells [7]. An enhanced mRNA expression of three type 2 DGAT genes changed neither the lipid content nor fatty acid profiles [8]. The knockdown or overexpression of five GPDH homolog genes showed that only GPDH2 and GPDH3 transgenic lines had significant lipid concentration and composition changes [4]. In addition, the enzymes regulating fatty acid metabolism such as acyl-ACP thioesterase (Fat), acetyl-CoA carboxylase (ACCase) and phosphoenolpyruvate carboxylase (PEPC) were also identified and proven to participate in biosynthesis of TAGs. The overexpression or silencing of these lipid metabolism-related genes in microalgae could change lipid contents and compositions often accompanied by a lower biomass and chlorophyll concentration, which indicated brakes in the biodiesel yield [9–11]. Therefore, in order to promote microalgae biodiesel production, it is necessary to uncover the mechanism of microalgae lipid biosynthesis.

Genomics, transcriptomics, proteomics and metabolomics analyses of *C. reinhardtii*, which is a model species for microalgae research, suggest that the TAG accumulation in microalgae is a complicated network system including key enzymes of lipid biosynthesis and transcriptional and post-transcriptional regulators [12,13]. The ubiquitin proteasome pathway (UPP) is a major regulatory network that permits eukaryote cells to integrate signals into a cellular response. In the UPP, highly conserved 76-amino acid protein ubiquitin (Ub) forms polymers by a three step (E1, E2 and E3) conjugation [14]. E3 ubiquitin ligases (E3s) confer the substrate specificity in ubiquitination. E3s have diverse functions in the eukaryote cell including the adjustment of the biosynthesis of lipids. It has been reported that in adipose tissue, E3 ubiquitin ligase constitutive photomorphogenic protein 1 (COP1) directly degrades ACCase, the rate-limiting enzyme in fatty acid synthesis, triggered by pseudokinase Tribbles 3 (TRB3) [15]. The survey of lipid droplets (LD) also showed that E3 ubiquitin ligase acts in an important regulatory way to control LD formation [16]. However, the current understanding of the roles of E3s in microalgae lipid metabolism is very limited.

Cullin assembles cullin-RING E3 ubiquitin ligase (CRL) complexes, which are the largest family of E3 ligases with more than 200 members [17]. The cullin family evolutionarily conserves in different species; e.g., there are seven human cullins, five Arabidopsis cullins and three yeast cullins [18]. In CRL complexes, cullin proteins often tether both a substrate-recognition subunit (SRS) through an adaptor protein and the RING finger component, which recruits an E2 ubiquitin-conjugating enzyme (Figure 1). CUL1 and CUL7 interact with SKP1 (S-phase kinase-associated protein 1) and F-box, commonly known as SCF, recruiting substrates through the adaptor protein SKP1 and F-box protein [19,20]. CUL2 and CUL5 bind to the elongin B/C in the suppressor of cytokine signaling/elongin-B/C (SOCS/B/C) boxes. CUL3 is specifically merged into a single 'Broad complex, Tramtrack, Bric-a-brac' (BTB) domain containing a polypeptide that assembles the adaptor and substrate receptor [21]. CUL4 links the substrate through the large protein DNA damage-binding protein-1 (DDB1), which binds to SRSs containing WD repeats of a subclass called 'DWD' [22]. Due to the reaction with RING Box 1 (RBX1) and modified by Ned8, the PARKin-like cytoplasmic protein (PARC) was defined as a cullin protein but its function is still unknown [16]. More mechanisms and roles of cullins in eukaryote cells need to be revealed in future.

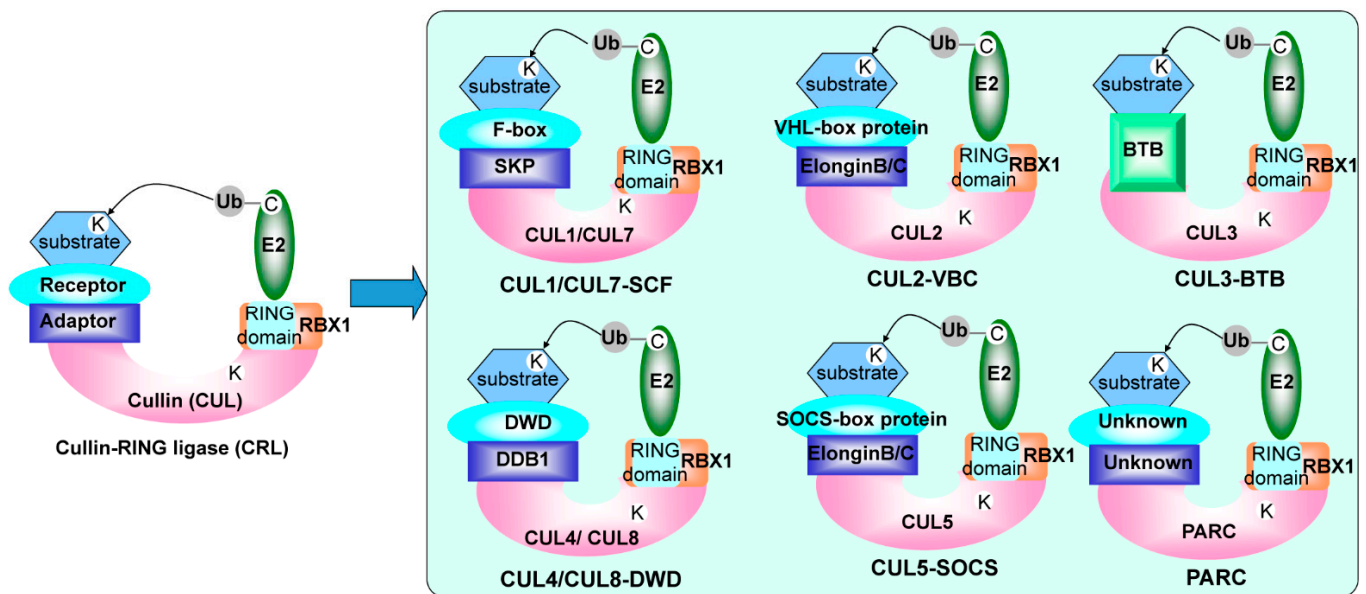


Figure 1. Diagram of cullin-RING ligases [17]. The C in the E2 presents the active site cysteine that binds to activated ubiquitin (Ub). The K in substrates and cullins indicates the acceptor sites for ubiquitin or Nedd8, respectively.

In *C. reinhardtii*, ubiquitin has been reported to play similar roles in response to various stresses. Using a yeast two-hybrid screening assay, CrCUL4 has been proven to interact with CrDDB1 to form a ligase complex that suppresses the expression of photoprotective genes in the dark [23]. However, the molecular roles of CrCULs underlying the lipid accumulation process are still a puzzle. Here, *Cullin* genes from *C. reinhardtii* were identified and then their gene expression profiles under nutrition deprivation were revealed. The RNAi expression vectors for three CrCULs were constructed and inserted into *C. reinhardtii* genomic DNA to obtain the gene inhibiting expression. Lipid contents and fatty acid (FA) profiles of CrCUL RNAi lines were surveyed to find out whether lipid biosynthesis in *C. reinhardtii* could be affected by CrCULs.

2. Results and Discussions

2.1. Cullins in *C. Reinhardtii*

The alignment sequences of the cullins E3 ubiquitin ligases (ID: PF00888) were obtained after searching in PFAM. Through Hmmssearch in *C. reinhardtii* proteome data with the cullins proteins as the queries, three CrCUL total sequences were obtained. Final cullins proteins obtained from the *C. reinhardtii* proteome in the Phytozome database were named as CrCUL2 (Cre17.g734400.t1.1), CrCUL3 (Cre07.g324050.t1.2) and CrCUL4 (Cre12.g516500.t1.1) based on the potential orthologs in Arabidopsis. The protein sequence characteristics are shown in Table 1. The length of the predicted CrCUL proteins were in the range of 736 (CrCUL3) and 766 aas (CrCUL4) and ORF lengths ranged from 2211 to 2301 bp. Moreover, the theoretical isoelectric point (pI) and the molecular weight of the CrCULs ranged from 6.98 to 8.49 and 84.8 to 87.6 kDa, respectively. Three CrCULs were hydrophilic proteins; among them, CrCUL4 and CrCUL2 had one and three possible transmembrane helices, respectively, while CrCUL3 had no transmembrane domain.

Table 1. List of three *CrCUL* genes identified in *C. reinhardtii* and their sequence characteristics.

Gene Name	Chromosome Position	Introns	ORF	Deduced Polypeptide				
				Amino Acids	MW (kDa)	pI	GRAVY	Transmembrane Helices
<i>CrCUL2</i>	17:4895502 ... 4903556F	19	2244	747	87.6	6.98	−0.214	3
<i>CrCUL3</i>	7:1516277 ... 1525175F	18	2211	736	84.8	8.14	−0.473	0
<i>CrCUL4</i>	12:3957943 ... 3963740F	14	2301	766	84.8	8.49	−0.576	1

ORF, open reading frame; MW, molecular weight; GRAVY, grand average of hydropathicity.

In recent years, cullin proteins in higher plants and animals have been well understood. Their special features and various functions have been well characterized. However, cullin proteins in green microalga were little known of to date. In this study, the *cullin* gene family in the *C. reinhardtii* genome was investigated by using cullin alignment sequences as queries. A total of three *CrCUL* homologue genes were isolated from the *C. reinhardtii* genome sequence and the gene numbers were different from those in higher plants but similar to those in fungi. An early phylogenetic analysis showed all CUL proteins were derived from three ancestral genes, *CUL α* , *CUL β* and *CUL γ* . Three identified *CrCULs* in the *C. reinhardtii* genome confirmed the primitive evolution status of *C. reinhardtii*. *CrCUL* genes are located on different chromosomes, which are similar to the *CULs* in *S. cerevisiae*. The lengths of *CrCULs* are 736 to 766 amino acids, which are similar to *AtCULs*. The length of the predicted ORFs and the amino acid sequences of all *CrCULs* are similar to *CULs* characterized in *Arabidopsis* [24]. Furthermore, both *CrCUL2* and *CrCUL4* have transmembrane helices, indicating that they might participate in molecular transmembrane transport.

Exons/intron structures of *CrCUL* genes were visualized by DAMMAN. As shown in Figure 2a, the three *CrCULs* contained 14–19 introns showing the complexity of the *C. reinhardtii* genome. All *CrCUL* proteins have domains typical for the cullin family, which include a cullin domain and an N-terminal Nedd8 domain (Figure 2b). A cullin domain at the C-terminal ends of cullins binding to RING proteins (Rbx1/ROC1) serves as the catalytic centers of CRL complexes while the Nedd8 domain at the N-terminal end promotes CRL activity through neddylation [25]. To examine the cullin domain features of *CrCUL* proteins, the sequence alignment was performed using MUSCLE (Figure 2c). Conserved amino acid residues of a cullin motif of *CrCULs* were highly homologous. These findings suggested that *CrCULs* encoded the cullins protein family in *C. reinhardtii*.

The phylogenetic tree based on the cullins protein sequence showed that cullins were evolutionarily conserved from human to yeast. *CrCUL2* and *CrCUL3* proteins clearly belong to the plant cullins branch (Figure 2d). However, *CrCUL4* protein as homologous with the animal cullins. A phylogenetic tree analysis revealed that *CrCUL2* and *CrCUL3* might have similar functions with *CULs* in plants, which play key roles in the control of photomorphogenesis and multiple developmental pathways [26]. The 3D model of *CrCULs* was constructed by Phyre2 based on a template human Cullin4a (PBD ID: c2hyeC, chain C, resolution of 7.40 Å) [27]. As shown in Figure 2e, *CrCUL2* and *CrCUL3* exhibited similar structures with the model identification of 53% and 39%, respectively, while *CrCUL4* had β -sheets at the N-terminal with a model identification of 37%. The strong similarity between the predicted three-dimensional structure of *CrCULs* (Figure 2e) and the cullin and Nedd8 domains confirmed that *CrCULs* belong to the cullin protein family.

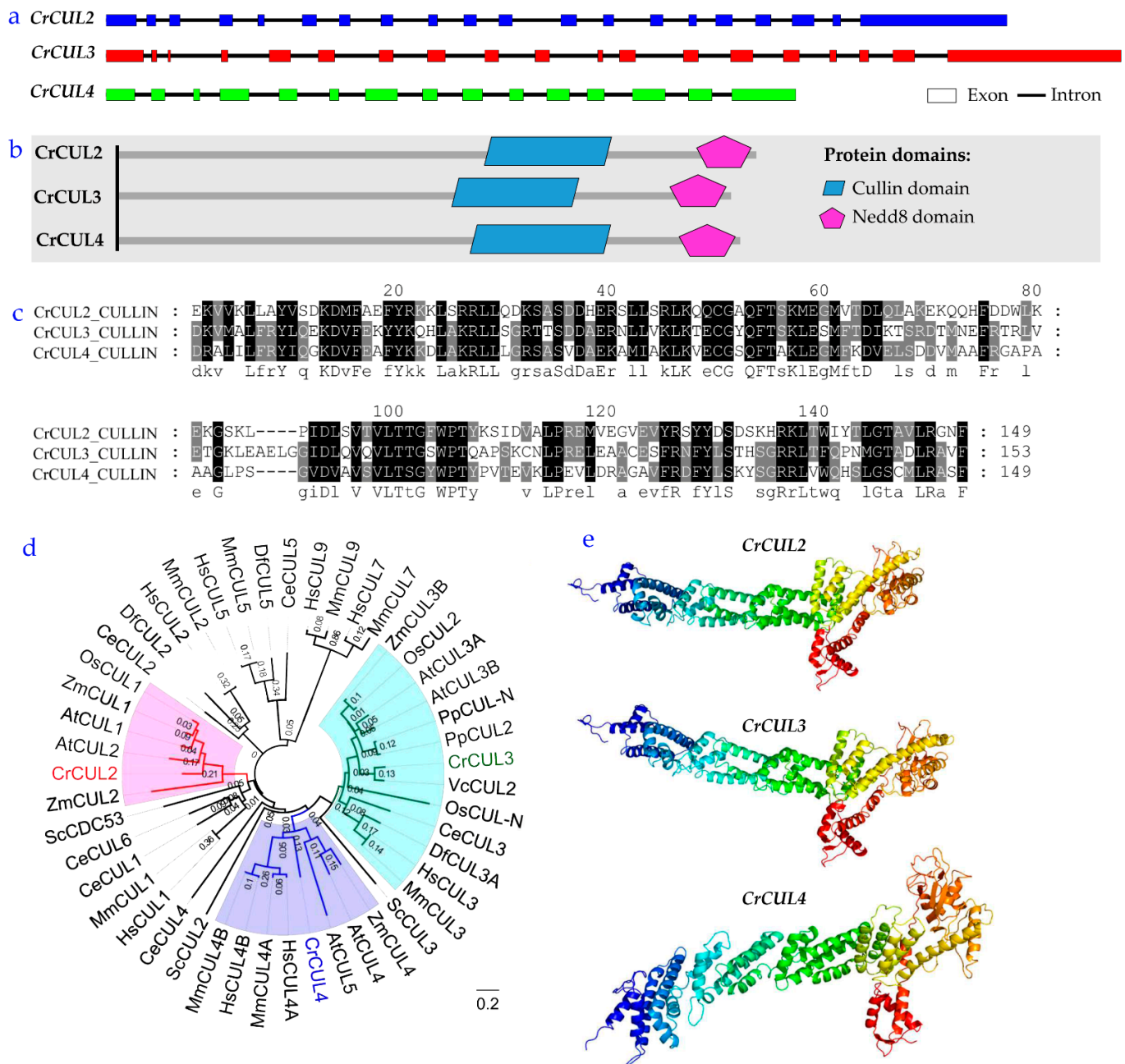


Figure 2. Sequence analysis of cullins in *C. reinhardtii*. (a) Gene structures of *CrCULs*; colored boxes indicate exons and lines show introns. (b) Conserved motif composition of *CrCULs*. The blue and purple boxes indicate cullin and nedd8 domains, respectively. (c) Sequence alignment of cullin domains of *CrCULs* using MUSCLE. Numbers show the positions of amino acid residues. Conserved residues are shown in black. (d) A phylogenetic tree of *CrCULs* was constructed using MEGA7.0. The phylogenetic tree was created by a neighbor-joining method and used 1000 bootstraps on the basis of the amino acid sequence of cullins from model organisms. Cr, *Chlamydomonas reinhardtii*; Hs, *Homo sapiens*; Mm, *Mus musculus*; Df, *Drosophila* fly; Ce, *Caenorhabditis elegans*; Vc, *Volvox carteri*; Sc, *Saccharomyces cerevisiae*; At, *Arabidopsis thaliana*; Os, *Oryza sativa*; Zm, *Zea mays*; Pp, *Physcomitrella patens*. (e) 3D model of *CrCULs* predicted by the Phyre2 software.

2.2. Expression Patterns of CrCUL Genes under Different Nutrition Deficiency Conditions

Previous studies showed that nutrition starvation was the most effective method to induce lipid accumulation in microalgae. Many key genes involved in lipid biosynthesis were revealed under nutrition deficiency conditions [28]. Here, in order to evaluate the expression patterns of CrCUL genes in response to nutrition deficiency, a quantitative real-time RT-PCR analysis with cells subjected to eight days of nutrition deprivation conditions such as nitrogen deficiency (-N), sulfur deficiency (-S) or iron deficiency (-Fe) was performed. The relative mRNA expression levels of CrCULs in stress treatment groups were calculated by normalizing with a control.

Nitrogen (N) and sulfur (S) are necessary macroelements for microalgal metabolism. The limitation of the supply of these elements has significant negative impacts on cell count, total protein and chlorophyll levels but lipid production increased by several folds more than the normal conditions [2]. Compared with the control, there was no change in the CrCUL2 gene expression level after N-deficient treatment for six days but a decline was observed at eight days (Figure 3a). CrCUL3 remarkably decreased and reached its lowest point (0.07-fold) after N was limited for two days then recovered gradually. The transcriptional level of CrCUL4 was significantly induced (2.43-fold) by N deficiency after two days but inhibited thereafter. Nitrogen is one of the important elements for *C. reinhardtii*. Under N stress, photosynthetic pigments were progressively lost and photosynthetic apparatus parallel decreased [29]. CUL3 in Arabidopsis modulates the phototropic responsiveness that mediates mono/multiubiquitination of *phot1* [30]. CUL4 also participates in higher plant photo morphogenesis. The transcriptional level changes of CrCUL3 and CrCUL4 during N deficiency indicated that they might mediate *C. reinhardtii* photomorphism. On the other hand, in the case of S deficiency, the CrCUL3 and CrCUL4 genes were induced dramatically (Figure 3b). The transcriptional level of CrCUL3 and CrCUL4 had peaks after 6 d and 8 d, respectively, which were 7.5 times and 6.9 times higher than that of the control. By contrast, the CrCUL2 gene was down-regulated by 49.2% after S deficiency treatment for eight days. Overall, CrCUL2 seemed insensitive to N and S deficiencies and exhibited a decrease after treatment for eight days. CrCUL3 obviously decreased under N deficiency but induced significantly under S deficiency (Figure 3a,b). Although CULs in higher plants have been isolated and their expression profiles under different lighting conditions have been identified in previous studies [31], a CUL gene expression analysis under nutrition deficiency is firstly revealed in this study.

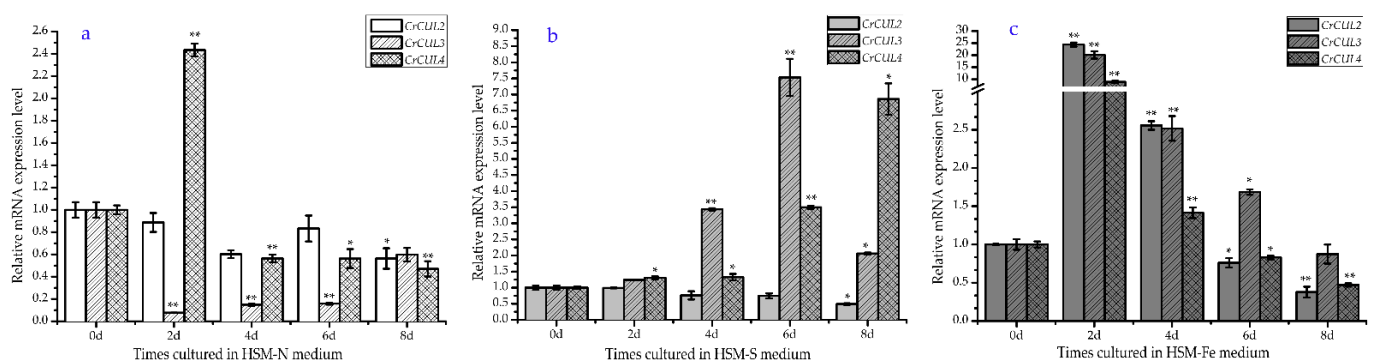


Figure 3. Expression patterns of CrCULs in *C. reinhardtii* under deficiency stresses for eight days. The relative expression levels of CrCULs under nutrition deprivation conditions including nitrogen (a), sulfur (b) and iron (c) deprivation were calculated. Each value represents the mean \pm standard error (SE) of the three replicates. * and ** indicate significant differences $p \leq 0.05$ and $p \leq 0.01$, respectively, according to Dunnett's analysis.

It was interesting to note that *CrCUL* genes shared similar expression patterns under iron deficiency conditions, which peaked after two days. The degrees of up-regulation then declined slightly (Figure 3c). Iron (Fe) is one kind of microelement for unicellular photosynthetic algae *C. reinhardtii*. Fe deficiency could obviously deduce the photosynthetic rate and photosynthesis-related proteins but could also induce the accumulation of TAG, which results in the formation of lipid droplets [32]. Previous studies have shown several members of Coat Protein Complex I (COP I) increased under metal deficiency/limitation conditions [33]. COP I is a WD40 repeat (WDR) domain containing E3 ubiquitin and often adapts with CUL4 to inhibit normal rates of lipid degradation [34]. However, the knowledge about the involvement of ubiquitin ligase under nutrition deficiency was limited. Here, dramatic increases in the level of *CrCULs* under iron deficiency were observed (Figure 3c), which implied the relation between *CrCULs* and metabolism under iron deficiency.

2.3. RNAi Expression of *CrCULs* in *C. reinhardtii*

C. reinhardtii CC425 was transformed with the p*Maa7IR* or p*Maa7IR-CrCUL* vectors in which dsRNA was generated from *CrCUL* cDNA fragments driven by a *CrRbcS* promoter. Positive transformants were grown under 5-fluorindol (5-FI) and paromomycin selective pressures. The RNAi expression lines of *CrCULs* were then determined by qRT-PCR randomly. The CC425 strains and p*Maa7IR* transformants were applied as controls (named as *Maa7* lines). The mostly inhibited *CrCUL* lines were confirmed as the RNAi lines and chosen for a further analysis. According to the results of the qRT-PCR assays, *CrCUL* RNAi lines were successfully constructed (Figure 4). Compared with the CC425 strains, the relative *CrCUL2* gene expressions in *CrCUL2*-i19 and *CrCUL2*-i35 lines decreased by 27.7% and 17.4%, respectively (Figure 4a). The related genes in the *CrCUL3*-i8 and *CrCUL3*-i44 strains were deprived by 20.2% and 11.3%, respectively (Figure 4b). The mRNA expressions of *CrCUL4* in the *CrCUL4*-i13 and *CrCUL4*-i57 lines were inhibited by 28.8% and 20.9%, respectively (Figure 4c) while related gene expressions in the p*Maa7IR* transformants (*Maa7s*) changed little. These data indicated that the *CrCUL* expression was significantly interfered with in the RNAi strains. RNAi strategies using a tandem inverted repeat (IR) system have been applied successfully in *Chlamydomonas* reverse genetic studies [35]. PEPC, DGAT2 and many other key enzymes in lipid synthesis have been characterized by the RNAi method [7]. The inhibitory efficiency of the above RNAi on mRNA levels of *CrCULs* suggested that the transgenic lines were suitable for a further analysis.

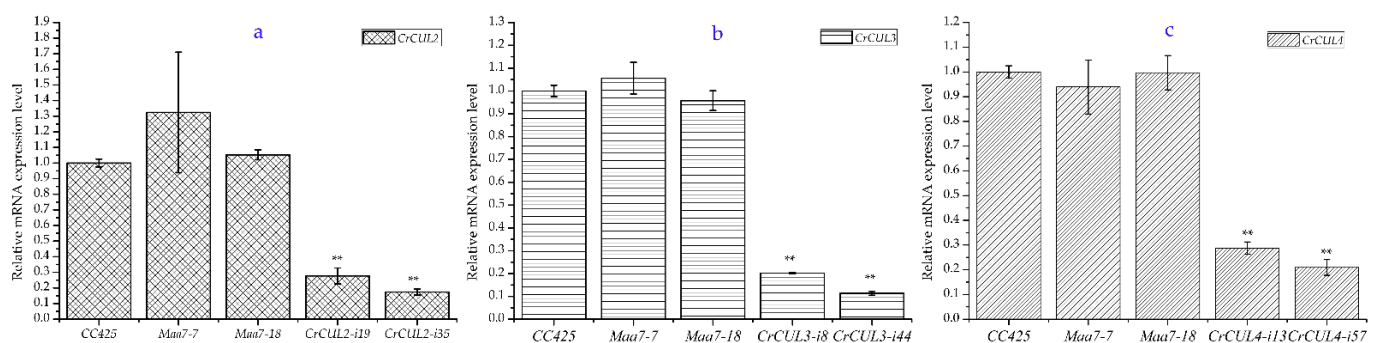


Figure 4. The expression levels of *CrCULs* decrease in RNAi transformants. Relative mRNA expression levels of *CrCULs* were analyzed by real-time RT-PCR analysis, (a) for the *CrCUL2* gene, (b) for the *CrCUL3* gene, (c) for the *CrCUL4* gene. Three experiments were performed with the CC425 strain as the control. Error bars indicate the standard deviation. The asterisks show statistically significant differences by Dunnett's multiple range test; ** $p \leq 0.01$.

2.4. Growth Kinetics and Lipid Contents of CrCUL RNAi Lines

To evaluate the effect of *CrCUL* gene silencing on cell growth, the successful *CrCUL* RNAi lines were selected for a growth kinetics analysis with the empty vector transformant (*Maa7-7* line) as the control. A similar seedling density (5×10^5 cells/mL) and equivalent sampling intervals were applied at the beginning. The cell density was measured during growth phase per day. After being cultured for three days, *CrCUL* mutants showed decreased cell densities, as shown in Figure 5a. Mutants *CrCUL3-i44* and *CrCUL4-i57* showed growth peaks at day seven while *CrCUL2-i35* and the control showed growth peaks at day six. After being grown for seven days, the *CrCUL2-i35* and *CrCUL4-i57* strains showed 28% and 34% less cell density than the control (Figure 5a), respectively, while the biomass productivity of *CrCUL3-i44* increased 1.12-fold compared with the *Maa7-7* strain at day eight. Although the *CrCUL3* and *CrCUL4* mutants showed varied growth profiles, their cell numbers became similar after 10 days of growth. Therefore, RNA silencing of *CrCUL* genes showed a negative effect on cell growth.

CRLs are major regulators of the cell cycle. For example, CRL1 complexes control cell proliferation and cell cycle progression by degrading cell cycle regulators binding to F-box proteins (FBP). Cul4-DDB1 ubiquitin ligase interacts with and degrades DNA replication factor Cdt1 controlling DNA replication [36]. CUL2 interacts with VHL (von Hippel-Lindau) and is required for a cell cycle G1-S period transition and for mitotic chromosome condensation [37]. At the same time, CUL4a CRL monoubiquitylates histone H2A acting in chromatin remodeling and CRL4 responds to DNA damage in metazoans and plants. Moreover, CRL3 binds to the BTB protein to participate in cell differentiation but not the cell cycle. The inhibition of *CrCUL2* and *CrCUL4* resulted in reduced cell numbers (Figure 5a) possibly because of the important roles of CUL2 and CUL4 in regulating the cell cycle. However, we were unable to speculate the reason for the irregular cell numbers of the *CrCUL3* RNAi lines.

CRLs have been demonstrated to control the formation of lipid droplets in mammals in past decades. In an attempt to understand the role of *CrCULs* in lipid synthesis regulation, we examined the lipid content in *CrCUL* RNAi strains. After two days of culture under similar environmental conditions, cells were collected for a lipid content analysis. Lipids in cells were stained by Nile red. The fluorescence intensity was converted into the lipid concentration according to the standard curve and then normalized by the cell density, as shown in Figure 5b. All three *CrCUL* gene silencing strains increased in lipid content compared with the control (*Maa7* empty vector transformant). However, the silencing mutant of *CrCUL3* exhibited a different curve pattern of a dynamic lipid content from *CrCUL2* and *CrCUL4*. Compared with the control, the silencing mutants of *CrCUL2* and *CrCUL4* constantly encouraged lipid biosynthesis in cells but the silencing mutant of *CrCUL3* did not exhibit any promotive effect on lipid content from day seven. The silencing mutants of *CrCUL2* and *CrCUL4* accumulated the highest lipid levels at day ten; approximately 1.28 and 1.20 times more than the control, respectively. By contrast, the first peak value of lipid content occurred at day five and a putative stationary phase of lipid content occurred thereafter in the silencing mutant of *CrCUL3*. Therefore, a conclusion that the biomass was inversely associated with the lipid contents in *CrCUL* mutants could be drawn. However, the role of *CrCUL3* seems to be different from *CrCUL2* and *CrCUL4*.

To observe the lipids in *CrCUL* RNAi lines, Nile red was used to bind to neutral lipids such as TAG in cells. The imaging results indicated that *CrCUL2-i35* and *CrCUL4-i57* cells accumulate more TAG than the control cells (Figure 5c), which agreed with the higher lipid contents detected by the fluorescence intensity. It was direct evidence for CULs participating in lipid formation that CUL3 in *LiSa-2* cells localized around LDs and the down-regulation of CUL3 and the inhibition of neddylation could block the formation of lipid droplets (LDs) [38]. However, after silencing the gene expression of *CrCULs*, the *CrCUL3* RNAi lines did not show constantly tremendous changes in lipid content. A possible reason is that CULs from plants and animals have different roles. Although the functions of CULs in higher plants have been demonstrated intensively, the

information of CULs in microalgae is very limited. So far, the photoprotective role of the E3 ubiquitin ligase CUL4-DDB1-DET1 complex, which mediates blue-light signals to the LHCSR1 and LHCSR3 gene expression in *C. reinhardtii*, has been determined by using a specific inhibitor for CRL4 [23]. Stress-response proteins LHCSR1 and LHCSR3 also could be induced by nutrient starvation, which is beneficial for lipid accumulation. The lipid metabolic regulation function of CrCUL2 and CrCUL4 found in this study is an important supplement for CRLs in microalgae. However, it still requires further investigation on how CUL proteins work.

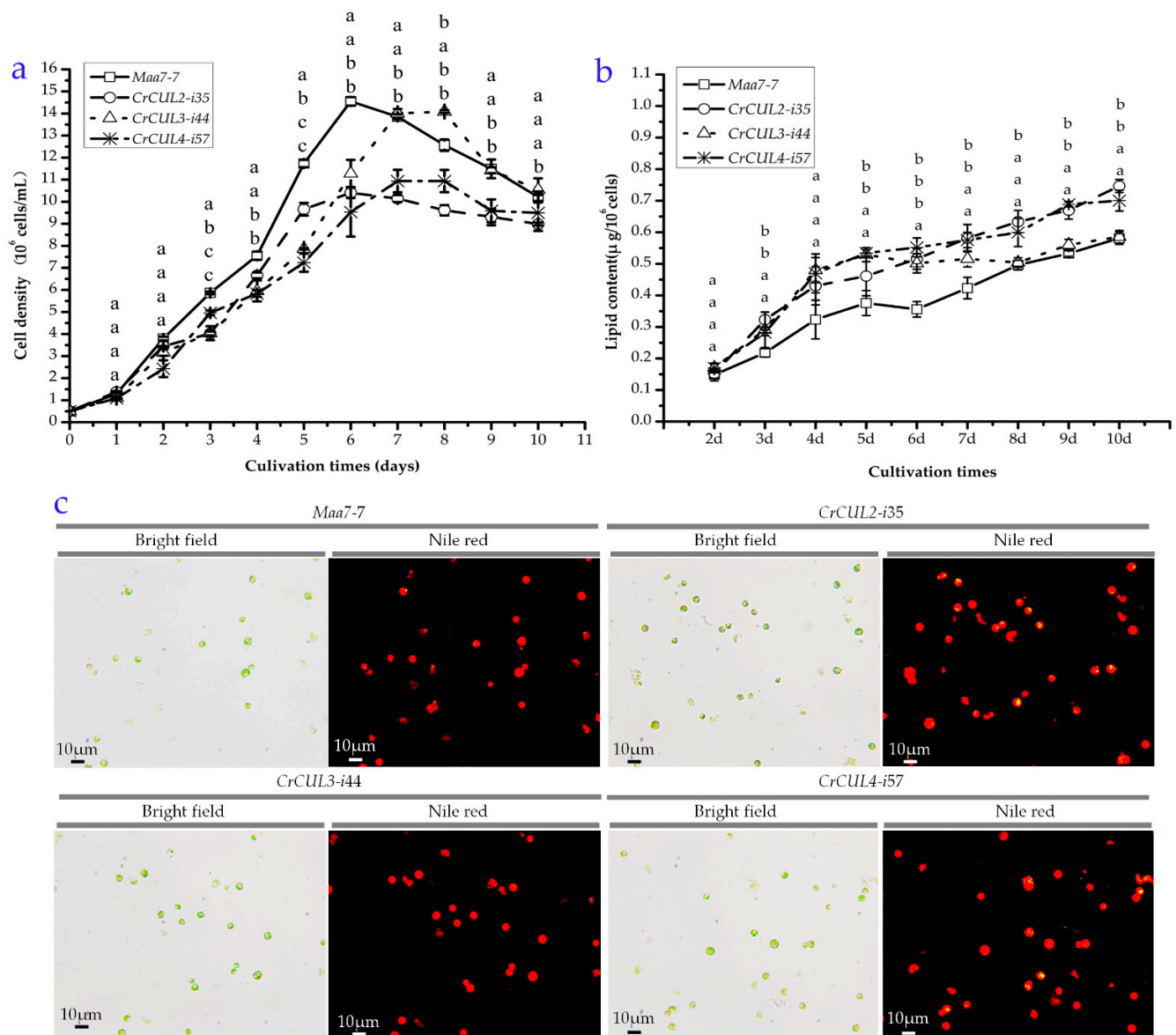


Figure 5. The growth and lipid accumulation of *CrCUL* RNAi lines. (a) The growth curve of *CrCUL* RNAi lines. Different letters indicate significant differences ($p \leq 0.05$) by Dunnett's multiple range test. (b) Total lipid contents of *CrCUL* RNAi lines. The lipid content of each strain was normalized to cell densities quantified at the growth phase. The data are representative of three replicas and different letters indicate significant differences ($p \leq 0.05$) by a one-way ANOVA. (c) TAG distubers in *CrCUL* RNAi lines and the control. Cells were grown in an HSM medium for 10 days. Lipid bodies were stained with Nile red (yellow dots) and imaged by fluorescence microscopy. Bar = 10 μm.

2.5. Fatty Acid Composition Analysis

Fatty acid (FA) composition is an important factor for biodiesel production. To illustrate the FA composition in the *CrCUL* RNAi lines, GC-MS was used to analyze the FA contents in transformants after 10 days of culture (Table 2). The highest total fatty acid (TFA) content was detected in the *CrCUL4-i57* line, i.e., 75.30 µg/mg, followed by *CrCUL2-i35* and *CrCUL3-i44*, which were 62.24 and 58.04 µg/mg, respectively. Only 55.19 µg/mg of TFA was detected in the control samples. Compared with the control group, TFA in *CrCUL2-i35*, *CrCUL3-i44* and *CrCUL4-i57* increased by 12.8%, 5.2% and 36.4%, respectively. The FA contents of *CrCUL3-i44* did not change significantly ($p > 0.05$), similar to its lipid contents. The increase in TFA content of the *CrCUL2-i35* strains was contributed by the increase of C16:0 and C18:0 fatty acids, which increased by 119.8% and 117.1%, respectively, compared with the control. C16:2 in the *CrCUL2-i35* cells decreased by 5.0% compared with the control. In the most TFA strain *CrCUL4-i57*, C16:0, C18:0, C18:3 (5, 9, 12), C18:3n3 and C20:0 had increases ranging from 130.7% to 154.15%. The results indicated that silencing *CrCUL2* and *CrCUL4* not only altered the TFA contents but also changed the FA composition.

Table 2. FA content (µg/mg) of *C. reinhardtii* *CrCUL* RNAi lines.

FA	<i>Maa7-7</i>	<i>CrCUL2-i35</i>	<i>CrCUL3-i44</i>	<i>CrCUL4-i57</i>
C12:0	0.04 ± 0.01	0.04 ± 0.00	0.03 ± 0.00	0.04 ± 0.00
C14:0	0.04 ± 0.01	0.12 ± 0.11	0.04 ± 0.00	0.05 ± 0.01
C16:0	12.25 ± 0.65 ^a	14.68 ± 0.89 ^b	11.28 ± 1.60 ^a	16.77 ± 1.47 ^c
C16:1	3.95 ± 0.11	3.45 ± 0.63	2.01 ± 0.68	4.55 ± 2.21
C16:2	1.21 ± 0.12 ^a	1.15 ± 0.20 ^b	2.00 ± 0.03 ^a	1.35 ± 0.19 ^a
C16:3	1.08 ± 0.36	0.80 ± 0.06	1.29 ± 0.11	1.35 ± 0.27
C16:4	4.68 ± 0.19	6.35 ± 2.53	7.66 ± 0.85	7.37 ± 2.04
C18:0	1.40 ± 0.12 ^a	1.64 ± 0.09 ^b	1.27 ± 0.09 ^a	1.83 ± 0.15 ^b
C18:1n9t	4.10 ± 0.40	4.77 ± 0.51	3.12 ± 1.13	4.44 ± 2.90
C18:1n9c	5.50 ± 0.54	5.88 ± 0.89	4.39 ± 0.56	6.85 ± 2.37
C18:2	5.74 ± 0.23	6.27 ± 0.52	7.45 ± 0.98	7.31 ± 1.59
C18:3 (5,9,12)	6.30 ± 0.32 ^a	6.47 ± 0.25 ^a	5.56 ± 0.74 ^a	9.65 ± 0.51 ^b
C18:3n3	8.20 ± 0.63 ^a	9.67 ± 2.35 ^a	10.81 ± 1.36 ^a	12.64 ± 3.16 ^b
C20:0	0.42 ± 0.03 ^a	0.50 ± 0.10 ^a	0.55 ± 0.03 ^a	0.63 ± 0.15 ^b
C20:1	0.26 ± 0.03 ^a	0.47 ± 0.31 ^a	0.60 ± 0.03 ^b	0.44 ± 0.16 ^a
Total FA	55.19 ± 0.92 ^a	62.24 ± 2.78 ^b	58.04 ± 2.11 ^a	75.30 ± 2.00 ^c

^{a,b,c}: Different letters of each line in the superscript position indicates they were significantly different at $p \leq 0.05$ according to a one-way ANOVA.

The modification of the FA synthesis pathways in microalgae was thought to be an effective strategy to improve the productivity of lipid synthesis. Research aimed at elevating the contents of fatty acids in microalgae strains for biofuel production have been performed for many years. Microalgae rate-limiting enzymes of an FA synthesis were analyzed and transferred to encourage lipid accumulation [9]. Nutritional polyunsaturated fatty acids (PUFAs), which are an important byproduct of microalgae, also need to be induced by genetic engineering. More recently, CRLs were reported to participate in fatty acid metabolism that a CUL3-MATH-BTB/POZ E3 ligases complex interacted with ETHYLENE RESPONSE FACTOR (ERF)/APETALA2 (AP2) transcription factors and thus altered fatty acid contents in Arabidopsis seeds [39]. Fatty acids C16:0 and C18:0, which are the main components for the preparation of biodiesel, were shown to be induced when *CrCUL2* and *CrCUL4* were silenced. Correspondingly, our results also demonstrated that *CrCUL2* and *CrCUL4* RNAi induced the accumulation of TFA and lipids (Figure 5 and Table 2). Based on the above results, we proposed that *CrCUL2* and *CrCUL4* might function as negative regulators in lipid biosynthesis by degrading a few key enzymes. In future, identifying the signaling pathways involving CrCRLs will be required.

2.6. Subcellular Localization of CrCUL4

CUL4-based E3 ligases (CRL4s) composed of CUL4, DDB1 and one WD40 protein have diversely important functions in cells. To determine its subcellular localization, CrCUL4 was inserted into a frame of a GFP reporter gene under the control of the cauliflower mosaic virus 35S (*CaMV 35S*) promoter. The recombinant *CrCUL4-GFP* fusion gene or the empty vector of pCAMBIA1302 were introduced into the *C. reinhardtii* CC124 strain by agrobacterium infection using kanamycin as the screening pressure. The positive colonies were chosen and observed by Olympus laser scanning confocal microscopy (LSCM). As shown in Figure 6, the CrCUL4-GFP fusion protein accumulated mainly in the nucleus whereas GFP alone was present throughout the whole cell, suggesting that CrCUL4 was a nucleus localized protein. In animals, CUL4 formed as a CRL4 complex, which is crucial for DNA replication and the cell cycle [40]. CUL4 conjugating with DDB1 in higher plants is located in the nuclear and is involved in multiple plant developmental processes [41]. A similar result in this study (Figure 6) showed that CrCUL4 may act at a chromatin level.

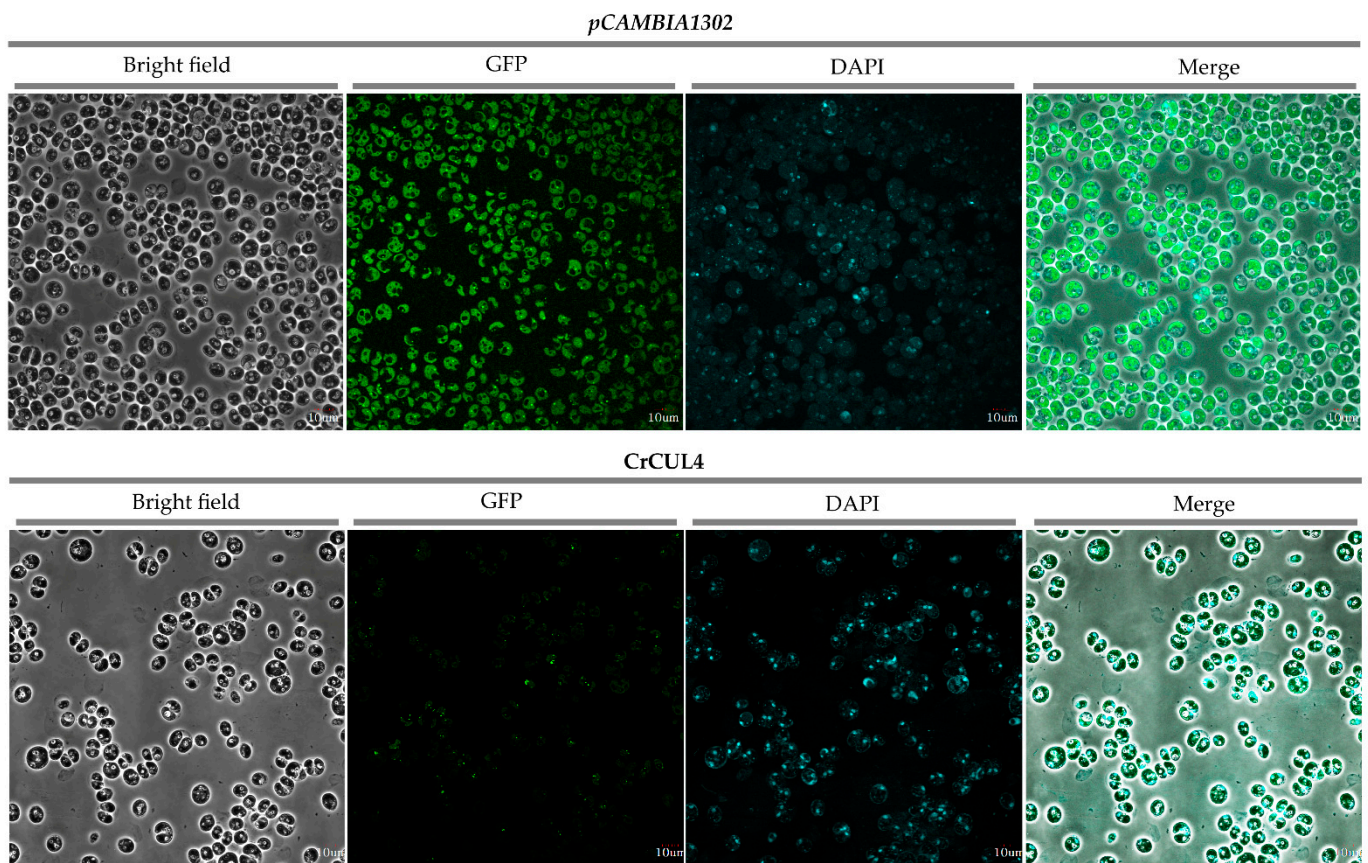


Figure 6. Localization of the CrCUL4-GFP protein. Individual panels show corresponding bright-field images, CrCUL4-GFP in *C. reinhardtii* CC124 cells and DAPI stained images and merged images, respectively. CrCUL4-GFP fusion was driven by the *CaMV 35S* promoter in vector pCAMBIA1302. Bars = 10 μ m.

3. Materials and Methods

3.1. In Silico Identification and Sequence Analysis of CrCULs

The seed sequences of alignments of the cullin protein family were identified in the PFAM (<https://pfam.xfam.org/>, accessed on 28 April 2021) database by searching with cullin as a keyword. An Hmsearch was performed in HMMER (<https://www.ebi.ac.uk/Tools/hmmer/search/hmmsearch>, accessed on 28 April 2021) *C. reinhardtii* proteomes used cullin proteins as query sequences, setting the E-value to less than 1×10^{-50} . Finally, all *C. reinhardtii* cullin sequences obtained from Hmsearch were analyzed by BLASTp using

version 5.5 of the *C. reinhardtii* proteome obtained from the Phytozome V12.1 database (<https://phytozome.jgi.doe.gov/pz/portal.html>, accessed on 28 April 2021). Only the sequences with an E-value cutoff of 1×10^{-50} were chosen as the candidate genes.

The intron/exon boundaries of *CrCUL* genes were shown by DNAMAN software. The motif analysis of the *CrCUL* proteins were verified by the SMART program (<http://smart.embl-heidelberg.de/>, accessed on 28 April 2021). Sequences of homologous proteins from model organisms were retrieved from NCBI (<https://www.ncbi.nlm.nih.gov/>, accessed on 28 April 2021) by blastp searching. A NJ phylogenetic tree of *CrCULs* was generated by Mega7.0 using a MUSCLE alignment with a bootstrap of 1000 replicates [42]. The phylogenetic tree was edited by FigTree v1.4.3 (<http://tree.bio.ed.ac.uk/software/figtree/>, accessed on 28 April 2021). The protein properties of the *CrCULs* including molecular weight, isoelectric point and hydrophobic properties were analyzed by ExPASy (<https://www.expasy.org/>, accessed on 28 April 2021). The transmembrane regions and orientation were predicted by TMPred (https://embnet.vital-it.ch/software/TMPRED_form.html, accessed on 28 April 2021). Comparative 3D protein predictions were performed using the Phyre2 (<http://www.sbg.bio.ic.ac.uk/phyre2/html>, accessed on 28 April 2021).

3.2. *C. reinhardtii* Strain and Growth Conditions

C. reinhardtii CC425 (cell wall deficient strain) was obtained from the College of Life Sciences and Oceanography of Shenzhen University (Shenzhen, China). Cells were grown under the following conditions: continuous illumination with an intensity of $25 \mu\text{mol photons}\cdot\text{m}^{-2}\cdot\text{s}^{-1}$ in 250 mL conical flasks containing 1/3 Tris-acetate-phosphate (TAP) media at 24 °C. For the gene expression analysis of *CrCULs*, cells in the logarithmic phase were collected and washed twice with fresh water by centrifugation at $3000 \times g$ for 5 min. After being washed, cells were transferred into either a low-nitrogen (-N), low-sulfur (-S) or low-iron (-Fe) medium grown for eight days and Sueoka's high salt medium (HSM) culture served as the control. The components of all media are listed in Table S1. Cells were collected by centrifugation, immediately frozen in liquid nitrogen after harvesting and then stored at $-80 \text{ }^\circ\text{C}$ until use.

For the transgenic experiment, cells were cultured to the logarithmic phase then collected and resuspended with a fresh TAP medium. Gene transfection was performed by the glassbeads method as described by Kindle et al. [43] and, after dark repair for 48 h, cells were plated on the selection media.

3.3. Gene Expression Analysis of *CrCULs*

Total RNA was isolated from -N, -S or -Fe cultured cells using a Trizol reagent (Invitrogen, Carlsbad, CA, USA). Genomic DNA contamination was erased and a first-strand cDNA synthesis by a PrimeScriptTM RT reagent kit with a gDNA Eraser (Takara, Kyoto, Japan) was used. Real-time RT-PCR was carried out in an Agilent StrataGene M \times 3005 (Agilent, Santa Clara, CA, USA) using a SYBR Premix Ex Taq Kit (Takara, Kyoto, Japan). The internal reference gene was set as the housekeeping gene *18S rRNA* (Genbank No: MF101220.1). The relative gene expression levels were calculated using the $2^{-\Delta\Delta\text{Ct}}$ method. Three biological replicates were performed for all relative abundances of an mRNA level analysis. All primers are listed in Table S2.

3.4. RNA Interference (RNAi) Vector Construction and Algae Transformation

To clone *CrCUL* genes, primer pairs (Table S2) were designed by Primer Premier 5.0 according to the predicted *CrCUL* coding sequences (CDS) obtained from the *C. reinhardtii* genome, version 5.5, in the Phytozome database. The cDNAs were generated from the total RNA of four day cultured cells with oligo dT primers using a PrimeScriptTM RT-PCR kit (Takara, Kyoto, Japan). A PCR was performed using the cDNA as the template. PrimeSTAR Max DNA Polymerase was applied with a protocol of 94 °C for 5 min, 35 cycles of 94 °C for 30 s, 56 °C for 1 min, 72 °C for 3 min 30 s and 72 °C for 10 min. The PCR products were purified and cloned into a pMD18-T vector (Takara, Kyoto, Japan) and then

sequenced by universal primers. The CDS of the *CrCUL4* gene were constructed into the pCambia1302 vector and transformed into the *CC124* for a subcellular location analysis. The positive colonies were observed by Olympus laser scanning confocal microscopy (Olympus, Kyoto, Japan).

The RNAi mediated silencing vectors of the *CrCUL* genes were constructed as described previously [44]. In brief, a 388 bp cDNA of *CrCUL2*, a 324 bp cDNA of *CrCUL3* and a 251 bp cDNA of *CrCUL4* were amplified from *CrCUL* CDS cloned by using primer pairs listed in Table S2. These fragments were inserted into the p*Maa7IR* silencing vector in a sense orientation and anti-sense orientation with restriction digestion and ligation. *CrCUL* RNAi vectors were transformed into the *C. reinhardtii* CC425 strain via the glass bead method. A TAP medium with 1.5 mM L-tryptophan, 5 µg/mL paromomycin and 5 µM 5-FI (Sigma-Aldrich, Saint Louis, MO, USA) was applied to select positive transgenic lines. The resistant colonies were picked up and the silencing efficiency of the *CrCUL* genes was detected by qRT-PCR.

3.5. Growth and Neutral Lipid Analysis

CrCUL RNAi transgenic strains and negative controls (p*Maa7IR*/X transgenic strains, shown as *Maa7* lines) were grown under normal conditions (HSM medium) as described above for 10 days. The cell density was measured using a Coulter™ Multisizer 4 (Beckman Coulter, Fullerton, CA, USA) every day.

For neutral lipid content (NL) examination, cells were stained by 0.5 µg/mL of Nile red (Sigma-Aldrich, Saint Louis, MO, USA) dissolved in 25% (*v/v*) of DMSO solution. The fluorescence intensity (FI) was measured with a Glomax-Multi Detection System (Promega, Madison, WI, USA) with excitation and emission wavelengths of 530 nm and 575 nm, respectively. Triolein (Sigma-Aldrich, Saint Louis, MO, USA) was used to make a standard curve. The neutral lipid content (NL) was calculated according to the formula:

$$\text{NL } (\mu\text{g}/10^6 \text{ cells}) = [(0.0004 \times \text{FI} (530/575) - 0.0038)] \times 50/\text{cell density} \quad (1)$$

The lipid accumulation in transgenic strains were observed by a Nikon 80 i fluorescence microscope (Nikon, Kyoto, Japan) after being stained with Nile red. The excitation and emission wavelengths of 480 nm and 580 nm were applied, respectively.

3.6. Fatty Acid Methyl Ester Profiling

After being cultured in HSM for 10 days, *CrCUL* RNAi lines and the controls were harvested by centrifugation and dried in a vacuum freezing machine. About 5–10 mg dry biomass were weighted for lipid extraction. First, 1 mL of a 2 M sodium hydroxide-methanol solution was added to cells, vigorously mixed by a shaker for 1 h and then saponified at 75 °C for 15 min. A total of 1 µg of methyl nonadecanoate (C15:0) was added as an internal standard for a gas chromatography-mass spectrometry (GC-MS) analysis. For fatty acid methyl-esterification, 1 mL of 4 M hydrochloric acid-methanol was added and incubated at 75 °C for 15 min. After cooling down, 1 mL of hexane was added into the vial to extract the methyl esters. The organic eluent was concentrated with nitrogen, diluted in 500 µL of CH₂Cl₂ and then analyzed by GC/MS Agilent 6890N (Agilent, Santa Clara, CA, USA).

3.7. Statistical Analysis

For comparisons of the means of *CrCUL* RNAi strains with the controls, a one-way analysis of variance (ANOVA), followed by a Dunnett's test was performed using the SPSS11.5 program. Data are shown as mean ± SD from three independent experiments unless specified otherwise. Significant differences between the controls and other samples are indicated as follows: the * indicate that they were significantly different at $p \leq 0.05$ and ** indicated $p \leq 0.01$ according to one-way ANOVA.

4. Conclusions

In summary, we demonstrated for the first time the regulating roles of three CrCULs in lipid synthesis in *Chlamydomonas*. A phylogenetic analysis showed CrCUL2 and CrCUL3 were homologous with plant CULs but CrCUL4 was more like the animal CULs. All CrCULs were transcriptionally induced by Fe deficiency for two days. The gene expression of CrCUL2 seemed to be insensitive to N and S deficiencies for six days. CrCUL3 was down-regulated by N-deficient conditions but up-regulated by S deficiencies. CrCUL4 expression was induced at two days after N-deficient treatment and then inhibited thereafter. After efficiently suppressing the expression of CrCUL genes by RNA interference, the RNAi of the CrCUL2 and CrCUL4 genes displayed a lower biomass but higher levels of lipid and TFA contents than the control. The significant alteration of lipid content and the composition of CrCUL mutants indicated that CrCULs play an important regulation role in lipid accumulation.

Supplementary Materials: The following tables are available online at <https://www.mdpi.com/article/10.3390/ijms22094695/s1>.

Author Contributions: Conceptualization, Q.L. and Z.H.; methodology, Q.L., X.Z. and Y.L.; software, Q.L.; data curation, Q.L. and X.Z.; project administration, Z.H.; writing—original draft preparation, Q.L. and Z.H.; writing—review and editing, X.Z., C.W.; and Z.H. All authors have read and agreed to the published version of the manuscript.

Funding: This work was supported by Chinese National Key R and D Project for Synthetic Biology (2018YFA0902500), National Natural Science Foundation of China (41876188, 31700309), Shenzhen Basic Research Projects (JCYJ20180507182405562), Guangxi Innovation Drive Development Special Fund (Gui Ke AA18242047), Funding for the Construction of Southern Marine Science and Engineering Guangdong Laboratory (Guangzhou) and Grant Plan for Demonstration City Project for Marine Economic Development in Shenzhen (No.86) to Zhangli Hu.

Institutional Review Board Statement: Not applicable.

Informed Consent Statement: Not applicable.

Data Availability Statement: Not applicable.

Acknowledgments: We thank additional lab personnel support provided by the Shenzhen Engineering Laboratory for Marine Algal Biotechnology.

Conflicts of Interest: The authors declare no conflict of interest.

Abbreviations

CRLs	Cullin-RING E3 ligases
CUL	Cullin
<i>C. reinhardtii</i>	<i>Chlamydomonas reinhardtii</i>
RNAi	RNA interference
TAG	Triacylglycerol
PDAT	Diacylglycerol acyltransferase
DGAT	Diacylglycerol acyltransferase
GPAT	Glycerol-3-phosphate acyltransferase
GPDH	Glycerol-3-Phosphate Dehydrogenases
Fat	Acyl-ACP thioesterase
ACCase	Acetyl-CoA carboxylase
PEPC	Phosphoenolpyruvate carboxylase
UPP	Ubiquitin proteasome pathway
E3s	E3 ubiquitin ligases
LD	Lipid droplets
SRS	Substrate-recognition subunit
SKP1	S-phase kinase-associated protein 1

SOCS/BC	Suppressor of cytokine signaling/elongin-BC
BTB	Broad complex, Tramtrack, Bric-a-brac
DDB1	DNA damage-binding protein-1
RBX1	RING Box 1
PARC	PARkin-like cytoplasmic protein
FA	Fatty acid
TAP	Tris Acetate Phosphate medium
HSM	Sueoka's High Salt Medium
-N	Nitrogen deficiency
-S	Sulfur deficiency
-Fe	Iron deficiency
COP I	Coat Protein Complex I
WDR	WD40 repeat domain
IR	Tandem inverted repeat
GFP	Green fluorescent protein

References

- Enamala, M.K.; Enamala, S.; Chavali, M.; Donepudi, J.; Yadavalli, R.; Kolapalli, B.; Aradhyula, T.V.; Velpuri, J.; Kuppam, C. Production of biofuels from microalgae—A review on cultivation, harvesting, lipid extraction, and numerous applications of microalgae. *Renew. Sustain. Energy Rev.* **2018**, *94*, 49–68. [\[CrossRef\]](#)
- Cakmak, T.; Angun, P.; Ozkan, A.D.; Cakmak, Z.; Olmez, T.T.; Tekinay, T. Nitrogen and sulfur deprivation differentiate lipid accumulation targets of *Chlamydomonas reinhardtii*. *Bioengineered* **2012**, *3*, 343–346. [\[CrossRef\]](#)
- Yoon, K.; Han, D.; Li, Y.; Sommerfeld, M.; Hu, Q. Phospholipid:diacylglycerol acyltransferase is a multifunctional enzyme involved in membrane lipid turnover and degradation while synthesizing triacylglycerol in the unicellular green microalga *Chlamydomonas reinhardtii*. *Plant Cell* **2012**, *24*, 3708–3724. [\[CrossRef\]](#)
- Driver, T.; Trivedi, D.K.; McIntosh, O.A.; Dean, A.P.; Goodacre, R.; Pittman, J.K. Two glycerol-3-phosphate dehydrogenases from *Chlamydomonas* have distinct roles in lipid metabolism. *Plant Physiol.* **2017**, *174*, 2083–2097. [\[CrossRef\]](#)
- Hung, C.H.; Ho, M.Y.; Kanehara, K.; Nakamura, Y. Functional study of diacylglycerol acyltransferase type 2 family in *Chlamydomonas reinhardtii*. *FEBS Lett.* **2013**, *587*, 2364–2370. [\[CrossRef\]](#)
- Herrera-Valencia, V.A.; Macario-Gonzalez, L.A.; Casais-Molina, M.L.; Beltran-Aguilar, A.G.; Peraza-Echeverria, S. In silico cloning and characterization of the glycerol-3-phosphate dehydrogenase (GPDH) gene family in the green microalga *Chlamydomonas reinhardtii*. *Curr. Microbiol.* **2012**, *64*, 477–485. [\[CrossRef\]](#)
- Deng, X.D.; Gu, B.; Li, Y.J.; Hu, X.W.; Guo, J.C.; Fei, X.W. The roles of acyl-CoA: Diacylglycerol acyltransferase 2 genes in the biosynthesis of triacylglycerols by the green algae *Chlamydomonas reinhardtii*. *Mol. Plant.* **2012**, *5*, 945–947. [\[CrossRef\]](#)
- Russa, M.L.; Bogen, C.; Uhmeyer, A.; Doebbe, A.; Filippone, E.; Kruse, O.; Mussgnug, J.H. Functional analysis of three type-2 DGAT homologue genes for triacylglycerol production in the green microalga *Chlamydomonas reinhardtii*. *J. Biotechnol.* **2012**, *162*, 13–20. [\[CrossRef\]](#)
- Tan, K.; Lee, Y.K. Expression of the heterologous *Dunaliella tertiolecta* fatty acyl-ACP thioesterase leads to increased lipid production in *Chlamydomonas reinhardtii*. *J. Biotechnol.* **2017**, *247*, 60–67. [\[CrossRef\]](#)
- Kao, P.H.; Ng, I.S. CRISPRi mediated phosphoenolpyruvate carboxylase regulation to enhance the production of lipid in *Chlamydomonas reinhardtii*. *Bioresour. Technol.* **2017**, *245*, 1527–1537. [\[CrossRef\]](#)
- Chen, D.; Yuan, X.; Liang, L.; Liu, K.; Ye, H.; Liu, Z.; Liu, Y.; Huang, L.; He, W.; Chen, Y.; et al. Overexpression of acetyl-CoA carboxylase increases fatty acid production in the green alga *Chlamydomonas reinhardtii*. *Biotechnol. Lett.* **2019**, *41*, 1133–1145. [\[CrossRef\]](#)
- Miller, R.; Wu, G.; Deshpande, R.R.; Vieler, A.; Gartner, K.; Li, X.; Moellering, E.R.; Zauner, S.; Cornish, A.J.; Liu, B.; et al. Changes in transcript abundance in *Chlamydomonas reinhardtii* following nitrogen deprivation predict diversion of metabolism. *Plant Physiol.* **2010**, *154*, 1737–1752. [\[CrossRef\]](#)
- Ramanan, R.; Kim, B.H.; Cho, D.H.; Ko, S.R.; Oh, H.M.; Kim, H.S. Lipid droplet synthesis is limited by acetate availability in starchless mutant of *Chlamydomonas reinhardtii*. *FEBS Lett.* **2013**, *587*, 370–377. [\[CrossRef\]](#)
- Small, J.; Vierstra, R.D. The ubiquitin 26S proteasome proteolytic pathway. *Annu. Rev. Plant Biol.* **2004**, *55*, 555–590. [\[CrossRef\]](#) [\[PubMed\]](#)
- Qi, L.; Heredia, J.E.; Altarejos, J.Y.; Screaton, R.; Goebel, N.; Niessen, S.; Macleod, I.X.; Liew, C.W.; Kulkarni, R.N.; Bain, J.; et al. TRB3 links the E3 ubiquitin ligase COP1 to lipid metabolism. *Science* **2006**, *312*, 1763–1766. [\[CrossRef\]](#) [\[PubMed\]](#)
- Thiele, C.; Spandl, J. Cell biology of lipid droplets. *Curr. Opin. Cell. Biol.* **2008**, *20*, 378–385. [\[CrossRef\]](#) [\[PubMed\]](#)
- Vierstra, Z.; Vierstra, R.D. The Cullin-RING ubiquitin-protein ligases. *Annu. Rev. Plant Biol.* **2011**, *62*, 299–334.
- Marín, I. Diversification of the cullin family. *BMC Evol. Biol.* **2009**, *9*, 267. [\[CrossRef\]](#)
- Roodbarkelari, F.; Bramsiepe, J.; Weinl, C.; Marquardt, S.; Novak, B.; Jakoby, M.J.; Lechner, E.; Genschik, P.; Schnittger, A. Cullin 4-ring finger-ligase plays a key role in the control of endoreplication cycles in *Arabidopsis* trichomes. *Proc. Natl. Acad. Sci. USA* **2010**, *107*, 15275–15280. [\[CrossRef\]](#)

20. Dias, D.C.; Dolios, G.; Wang, R.; Pan, Z.Q. CUL7: A DOC domain-containing cullin selectively binds Skp1.Fbx29 to form an SCF-like complex. *Proc. Natl. Acad. Sci. USA* **2002**, *99*, 16601–16606. [[CrossRef](#)]
21. Yin, C.Y.; Thilo, H.; Karl-Wilhelm, K. Mechanism of Cullin3 E3 Ubiquitin Ligase Dimerization. *PLoS ONE* **2012**, *7*, e41350.
22. Dumbliuskas, E.; Lechner, E.; Jaciubek, M.; Berr, A.; Pazhouhandeh, M.; Alioua, M.; Cognat, V.; Brukhin, V.; Koncz, C.; Grossniklaus, U.; et al. The Arabidopsis CUL4-DDB1 complex interacts with MSI1 and is required to maintain MEDEA parental imprinting. *EMBO J.* **2011**, *30*, 731–743. [[CrossRef](#)] [[PubMed](#)]
23. Aihara, Y.; Fujimura-Kamada, K.; Yamasaki, T.; Minagawa, J. Algal photoprotection is regulated by the E3 ligase CUL4-DDB1DET1. *Nat. Plants* **2018**, *5*, 34–40. [[CrossRef](#)]
24. Sarikas, A.; Hartmann, T.; Pan, Z.Q. The cullin protein family. *Genome Biol.* **2011**, *12*, 220. [[CrossRef](#)]
25. Hannah, J.; Zhou, P. Distinct and overlapping functions of the cullin E3 ligase scaffolding proteins CUL4A and CUL4B. *Gene* **2015**, *573*, 33–45. [[CrossRef](#)] [[PubMed](#)]
26. Dieterle, M.; Thomann, A.; Renou, J.P.; Parmentier, Y.; Cognat, V.; Lemonnier, G.; Muller, R.; Shen, W.H.; Kretsch, T.; Genschik, P. Molecular and functional characterization of Arabidopsis Cullin 3A. *Plant J.* **2005**, *41*, 386–399. [[CrossRef](#)]
27. Fischer, E.S.; Scrima, A.; Bohm, K.; Matsumoto, S.; Lingaraju, G.M.; Faty, M.; Yasuda, T.; Cavadini, S.; Wakasugi, M.; Hanaoka, F.; et al. The molecular basis of CRL4DDB2/CSA ubiquitin ligase architecture, targeting, and activation. *Cell* **2011**, *147*, 1024–1039. [[CrossRef](#)]
28. Lv, H.; Qu, G.; Qi, X.; Lu, L.; Tian, C.; Ma, Y. Transcriptome analysis of *Chlamydomonas reinhardtii* during the process of lipid accumulation. *Genomics* **2013**, *101*, 229–237. [[CrossRef](#)]
29. Wase, N.; Black, P.N.; Stanley, B.A.; DiRusso, C.C. Integrated quantitative analysis of nitrogen stress response in *Chlamydomonas reinhardtii* using metabolite and protein profiling. *J. Proteome Res.* **2014**, *13*, 1373–1396. [[CrossRef](#)]
30. Roberts, D.; Pedmale, U.V.; Morrow, J.; Sachdev, S.; Lechner, E.; Tang, X.; Zheng, N.; Hannink, M.; Genschik, P.; Liscum, E. Modulation of phototropic responsiveness in Arabidopsis through ubiquitination of phototropin 1 by the CUL3-Ring E3 ubiquitin ligase CRL3NPH3. *Plant Cell* **2011**, *23*, 3627–3640. [[CrossRef](#)]
31. Christians, M.J.; Rottier, A.; Wiersma, C. Light regulates the RUBYlation levels of individual Cullin proteins in *Arabidopsis thaliana*. *Plant Mol. Biol. Rep.* **2018**, *36*, 123–134. [[CrossRef](#)]
32. Devadasu, E.; Chinthapalli, D.K.; Chouhan, N.; Madireddi, S.K.; Rasineni, G.K.; Sripadi, P.; Subramanyam, R. Changes in the photosynthetic apparatus and lipid droplet formation in *Chlamydomonas reinhardtii* under iron deficiency. *Photosynth. Res.* **2019**, *139*, 253–266. [[CrossRef](#)] [[PubMed](#)]
33. Hsieh, S.I.; Castruita, M.; Malasarn, D.; Urzica, E.; Erde, J.; Page, M.D.; Yamasaki, H.; Casero, D.; Pellegrini, M.; Merchant, S.S.; et al. The proteome of copper, iron, zinc, and manganese micronutrient deficiency in *Chlamydomonas reinhardtii*. *Mol. Cell. Proteom.* **2013**, *12*, 65–86. [[CrossRef](#)] [[PubMed](#)]
34. Beller, M.; Sztalryd, C.; Southall, N.; Ming, B.; Oliver, B. CopI complex is a regulator of lipid homeostasis. *PLoS Biol.* **2008**, *6*, e292. [[CrossRef](#)] [[PubMed](#)]
35. Rohr, J.; Sarkar, N.; Balenger, S.; Jeong, B.R.; Cerutti, H. Tandem inverted repeat system for selection of effective transgenic RNAi strains in *Chlamydomonas*. *Plant J.* **2004**, *40*, 611–621. [[CrossRef](#)]
36. Teixeira, L.K.; Reed, S.I. Ubiquitin ligases and cell cycle control. *Annu. Rev. Biochem.* **2013**, *82*, 387–414. [[CrossRef](#)]
37. Feng, H.; Zhong, W.; Punkosdy, G. CUL-2 is required for the G1-to-S-phase transition and mitotic chromosome condensation in *Caenorhabditis elegans*. *Nat. Cell Biol.* **1999**, *1*, 486–492. [[CrossRef](#)] [[PubMed](#)]
38. Dubiel, D.; Bintig, W.; Kähne, T.; Dubiel, W.; Naumann, M. Cul3 neddylation is crucial for gradual lipid droplet formation during adipogenesis. *BBA Mol. Cell Res.* **2017**, *1864*, 1405–1412. [[CrossRef](#)]
39. Chen, L.; Lee, J.H.; Weber, H.; Tohge, T.; Witt, S.; Roje, S.; Fernie, A.R.; Hellmann, H. Arabidopsis BPM proteins function as substrate adaptors to a cullin3-based E3 ligase to affect fatty acid metabolism in plants. *Plant Cell* **2013**, *25*, 2253–2264. [[CrossRef](#)]
40. Kansanen, E.; Jyrkkanen, H.K.; Levonen, A.L. Activation of stress signaling pathways by electrophilic oxidized and nitrated lipids. *Free Radic. Biol. Med.* **2012**, *52*, 973–982. [[CrossRef](#)]
41. Zhang, Y.; Feng, S.; Chen, F.; Chen, H.; Wang, J.; Mccall, C.; Xiong, Y.; Deng, X.W. Arabidopsis DDB1-CUL4 associated factor1 forms a nuclear E3 ubiquitin ligase with DDB1 and CUL4 that is involved in multiple plant developmental processes. *Plant Cell* **2008**, *20*, 1437–1455. [[CrossRef](#)] [[PubMed](#)]
42. Faull, S.V.; Lau, A.M.C.; Martens, C.; Ahdash, Z.; Hansen, K.; Yebenes, H.; Schmidt, C.; Beuron, F.; Cronin, N.B.; Morris, E.P.; et al. Structural basis of Cullin 2 RING E3 ligase regulation by the COP9 signalosome. *Nat. Commun.* **2019**, *10*, 3814. [[CrossRef](#)] [[PubMed](#)]
43. Kindle, K.L. High-frequency nuclear transformation of *Chlamydomonas reinhardtii*. *Proc. Natl. Acad. Sci. USA* **1990**, *87*, 1228–1232. [[CrossRef](#)]
44. Luo, Q.; Song, W.; Li, Y.; Wang, C.; Hu, Z. Flagella-Associated WDR-Containing Protein CrFAP89 Regulates Growth and Lipid Accumulation in *Chlamydomonas reinhardtii*. *Front. Plant Sci.* **2018**, *9*, 691. [[CrossRef](#)] [[PubMed](#)]